Wiley
Journal of Engineering
Volume 2024, Article ID 5808787, 13 pages
https://doi.org/10.1155/2024/5808787

WILEY

Research Article

Transient Characteristics and Performance of a Dual Compensation Chamber Loop Heat Pipe under Various Heat Loads

P. Mohanraj,[1] **R. Sridhar**,[2] **T. Gopalakrishnan**,[2] **R. Manikandan**,[3] **and Abhijit Bhowmik**[4,5]

[1]*Department of Aeronautical Engineering, Jaya Engineering College, Thiruninravur, Chennai 602024, Tamil Nadu, India*
[2]*Department of Mechanical Engineering, Vels Institute of Science, Technology and Advanced Studies, Chennai 600117, Tamil Nadu, India*
[3]*Department of Mechanical Engineering, Saveetha School of Engineering, Saveetha Institute of Medical and Technical Sciences, Saveetha University, Chennai 602105, Tamil Nadu, India*
[4]*Department of Mechanical Engineering, Dream Institute of Technology, Kolkata 700104, India*
[5]*Centre of Research Impact and Outreach, Chitkara University, Rajpura 140417, Punjab, India*

Correspondence should be addressed to Abhijit Bhowmik; abhijit.bhowmik@dreaminstituteonline.com

Received 3 May 2024; Accepted 5 September 2024

Academic Editor: Tabish Alam

The dual compensation chamber loop heat pipe (DCCLHP) technology shows great promise for efficient thermal management in a variety of applications. This study focuses on refining the startup performance of the DCCLHP, particularly for low heat load conditions in terrestrial settings, by utilizing dual bayonet tubes. Empirical investigations examined the DCCLHP's operational characteristics and improved thermal transfer capabilities across different orientations of the evaporator and compensation chamber (CC), including vertical, 45-degree tilt angle, and horizontal configurations. Key results demonstrate the DCCLHP's ability to manage low heat loads across diverse orientations, achieving over 400 W of heat transfer across a distance of 2.0 m while maintaining stable operation. Notably, the DCCLHP operation did not exhibit any significant instability issues. This work enhances the startup performance of the DCCLHP in various orientations and provides valuable insights into the confined natural circulation phenomenon, crucial for improving the overall thermal management capabilities of the system. In summary, the study highlights advancements in DCCLHP design and its potential to address thermal management challenges in diverse applications, particularly in the aerospace industry, through improved startup performance and enhanced heat transfer capabilities.

1. Introduction

Effective thermal regulation is critical to aviation systems, ensuring optimal performance and safety. The dynamic and diverse operating conditions in aviation demand sophisticated thermal management solutions to prevent overheating, ensure component longevity, and maintain operational efficiency [1]. Incorporating loop heat pipes (LHPs) in thermal performance equipment with two-phase heat transfer has demonstrated significant efficacy. The DCCLHP emerges as a beacon of hope in the realm of aviation thermal management, drawing upon the essence of dual-phase heat transfer. Through skillful utilization of this concept, the DCCLHP presents a gateway to overcoming the multifaceted hurdles brought forth by diverse heat loads, orientations, and environmental circumstances within aviation infrastructures. With a blueprint that includes evaporators, compensation chambers (CCs), and a network of intricate fluid pathways, its design harbors the promise of effective heat dispersion and precise temperature control.

A loop heat pipe (LHP) is typically configured with an evaporator, a collector, a CC, and mechanisms that promote

vapor-liquid contact. This type of arrangement is considered conventional in heat pipe technology [2]. Liquid connection lines link to the bayonet tube for capacitor output, while the steam transport line connects steam grooves to the capacitor interface. A meniscus is produced when liquid heat pipes (LHPs) are introduced because they start the process of liquid evaporation in the wick's topmost layer. The capillary pressure this meniscus creates drives vapor via vapor grooves and transport lines into the condenser [3]. Condensation occurs during this phase, which results in the release of heat. The concentrated mixture returns to the liquid transport system to complete the cycle guided back toward the evaporative unit [4].

LHP offers distinct advantages, including efficient heat transfer over long distances and robust gravitational resistance, setting it apart from conventional heat pipes [5]. Moreover, its adaptable transport lines afford remarkable flexibility in installation and layout for potential applications [6]. Initially developed for spacecraft temperature management, LHPs have successfully resolved intricate thermal organization challenges in numerous space missions [7]. This technology has become a standard for spacecraft heat management. The capillary pumping system of LHP ensures dependable temperature control and heat dissipation. With ongoing technological advancements and maturation, LHP's utilization in space temperature control has expanded to diverse domains, including air temperature control. However, changes in aircraft attitude may hinder fluid flow to the evaporator wick, causing LHP operation disruptions [8].

Incorporating secondary wick hydro alongside the central wick and CC has been attempted to ensure continuous liquid supply to the evaporator under adverse conditions [9]. The traditional approach of using a secondary wick in loop heat pipes often results in a significant reduction in the heat transfer capacity, primarily due to the increased resistance to fluid flow. To address this issue, a novel solution known as the DCCLHP was developed. The DCCLHP integrates dual compensation chambers at the ends of the evaporator, which helps to overcome the limitations associated with the increased flow resistance in the secondary wick. This design innovation allows the DCCLHP to maintain efficient heat transfer capabilities while addressing the challenges posed by the traditional loop heat pipe configurations.

This design ensures adequate water supply to the evaporator wick regardless of orientation, making DCCLHP suitable for various landscape environments, including energy storage systems for aircraft [10]. Maydanik et al. [11] analyzed LHPs with various evaporator shapes, revealing optimal configurations and material combinations for enhanced performance. Maydanik [12] provided a comprehensive overview of LHPs, emphasizing their unique ability to efficiently transfer heat over varying distances and orientations, with significant applications in space technology and electronics. Ambirajan et al. [13] presented a comprehensive review of LHP fundamentals, design, and modeling, highlighting their application versatility in spacecraft thermal control, avionics cooling, and beyond. These studies underscore the remarkable potential of LHPs in addressing complex thermal management challenges across diverse technological domains.

Nakamura et al. [14] investigated long-distance LHPs under antigravity conditions, revealing their efficient heat transport over 10 m distances and evaluating the influence of gravity on thermal resistance and transfer efficiency [15]. In their recent study, Odagiri and Nagano [16] explored the thermal fluid dynamics in LHP evaporators. Their research has established a precise quantitative correlation between the behavior of the liquid-vapor interface and the facilitation of heat transfer at elevated flux levels. Maydanik et al. [17] showcased the potential of lengthy LHPs for diverse applications, highlighting impressive heat load capabilities and thermal resistance performance.

Arya et al. [18] investigated the intriguing use of ethylene glycol with MgO/water nanofluids in a sophisticated heat exchanger. Their results show a considerable improvement in hydraulic performance and heat transfer coefficients while concurrently resolving the problem of nanoparticle contamination. Guo et al. [19] delved deeply into the exploration and enhancement of a heat pump cycle utilizing CO2, designed to provide both heating and cooling simultaneously. The study presents valuable suggestions for enhancing system efficiency and promoting energy conservation. Guo et al. [19] delved into the properties of noncondensable gases on the initial operation of loop heat pipes. Moreover, the significance of this occurrence was evaluated in different situations pertaining to the dissemination of fluid and vapor in the evaporator. The authors' findings offer valuable insights and recommendations for effectively addressing the challenges of initiating loop heat pipe operations in space and terrestrial environments. Ramasamy et al. [20] reported the thermal behavior and orientation independence of a miniature ammonia loop heat pipe to evaluate its suitability for terrestrial applications. The investigation sought to establish the heat pipes' capacity to operate optimally under different orientations. They achieved a maximum capacity of 225 W with minimal thermal resistance and validated their mathematical model.

Xue et al. [21] conducted a novel study on an ammonia-pulsating heat pipe, visually capturing unique thermodynamic behaviors during startup and observing phenomena like circulation flows and slug-train distribution. Zhou and colleagues [22] introduced a compact loop heat pipe cooler featuring a slim flat evaporator, showcasing reliable initial operation and effective heat dispersion for mobile electronic devices. Additionally, a detailed analysis was conducted to enhance the assessment of its performance. Using loop heat pipes (LHPs) as the foundation, Bai et al. [23] created a power-free cooling system that used their effective long-distance heat transmission capabilities. The LHP's cylindrical evaporator was linked to a film heater via an aluminum saddle in their arrangement. In addition, a condenser line built into a fin radiator made it easier for heat to be removed by natural air convection.

The experimental findings demonstrated that the system was able to effectively dissipate heat, achieving a heat dissipation of 150 W over a distance of 1.05 m with a thermal resistance of around 0.30°C/W. This indicates that the system was able to efficiently transfer and dissipate the

generated heat, suggesting a successful thermal management design. The cooling mechanism exhibited a sturdy capability to counteract gravitational forces, functioning seamlessly even at an altitude of 0.5 meters [24]. This development provides valuable prospects for forthcoming utilization. In a separate study, they investigated compact copper-water LHPs with flat plate evaporators, comparing configurations with single and dual parallel condensers. Findings indicated that the LHP featuring dual parallel condensers achieved higher maximum heating power (1700 W) and lower total thermal resistance (0.067°C/W) under forced air cooling while also highlighting the need for further understanding of fluid distribution dynamics at lower heat loads in such setups [25]. The literature review underscores the significance of loop heat pipes in various applications, introduces the innovative design and components of the DCCLHP, and highlights prior research efforts to enhance startup behavior and optimize thermal performance. This body of knowledge is a foundation for the present study's exploration and advancement of the DCCLHP technology.

2. Materials and Methods

2.1. Materials. Propylene (C3H6) was considered a base fluid for DCCLHP setup due to its effectiveness across a temperature range from −20°C to +80°C [23]. The experimental setup of DCCLHP comprised different components such as the evaporator, compensation chambers (CC1 and CC2), vapor line, bayonet, condenser, and liquid line. A convoluted condenser tube was joined to an aluminum plate featuring fins to enhance the heat transfer surface area, while the aluminum plate was subjected to cooling through natural convection of air. In this instance, the ambient air acted as a heat sink, collecting heat from the condensation chamber and enabling the ambient temperature to be used as the heat sink temperature. The evaporator system, including the DCCLHP (loop heat pipe), compensation chambers (CC1 and CC2), vapor line, condenser, and liquid lines, is constructed using stainless steel, while the wick material is nickel.

2.2. Loop Heat Pipe Configuration. The experimental LHP system comprises several key components arranged in a specific configuration [26]. Figure 1 illustrates the detailed experimental setup of the DCCLHP system, which includes key components such as the evaporator, compensation chambers, vapor line, condenser, liquid line, and wing model.

(1) Evaporator: This is the core component where the working fluid absorbs heat. It is connected to two compensation chambers (CC1 and CC2), ensuring a stable supply of working fluid irrespective of the system's orientation. The evaporator has an outlet that connects to the vapor line.

(2) Compensation Chambers (CC1 and CC2): These compartments are linked to both ends of the evaporator, serving a vital function in regulating the delivery of the working substance to the evaporator and controlling the operational pressures present in the system.

(3) Vapor Line: The heated vapor from the evaporator is transported through this line to the condenser.

(4) Condenser: Located at the termination of the gaseous phase pathway, this component is tasked with converting the vapor into its original liquid form, consequently discharging the heat that was previously taken in.

(5) Liquid Line: This line carries the condensed liquid rear side to the evaporator, completing the heat transfer cycle.

(6) Wing Model: The wing model is an additional component used to simulate the application of the LHP in an aviation context. It is used to examine the heat transfer capabilities of the LHP when applied to aircraft components.

The evaporator has an outer diameter (O.D.) of 52 mm, an inner diameter (I.D.) of 45 mm, and a length (L) of 120 mm. It features 11 vapor grooves, each with a length of 1 mm and a width of 1 mm. The vapor and liquid lines both have an O.D. of 3 mm, an I.D. of 2 mm, and a length of 500 mm. The condenser has the same dimensions as the vapor and liquid lines. The wick material has a porous radius of 1.2 μm. The first compensation chamber (CC1) has a volume of 59.5 ml, and the second compensation chamber (CC2) also has a volume of 59.5 ml.

2.3. Temperature Measurement. To accurately assess the performance of the LHP, temperature sensors are strategically placed at several points:

(i) T_ein and T_eout: Measure the input and output temperatures of the evaporator.

(ii) T_cin and T_cout: Monitor the input and output temperatures of the condenser.

(iii) T_ec1, T_ec2, T_ec3, T_ec4: Positioned to measure temperatures at distinct positions throughout the compensation chambers.

2.4. Inner Structure. The internal design of the LHP is critical for its function:

(i) Wick Structure: Within the evaporator enclosure, a wick configuration enables the capillary pressure necessary for the movement of the operational fluid.

(ii) Vapor Grooves: The ridges facilitate the passage of vapor from the evaporation to the condensation.

(iii) Connecting Pipes: The evaporator and compensation chambers are linked by a network of pipes designed to facilitate the movement of both the working fluid and vapor.

2.5. Evaporator Casing and Wick Design. A perpendicular peek inside the evaporator housing unveils the intricate wick arrangement, crucial for the flow of the operational liquid and the effective functioning of the LHP.

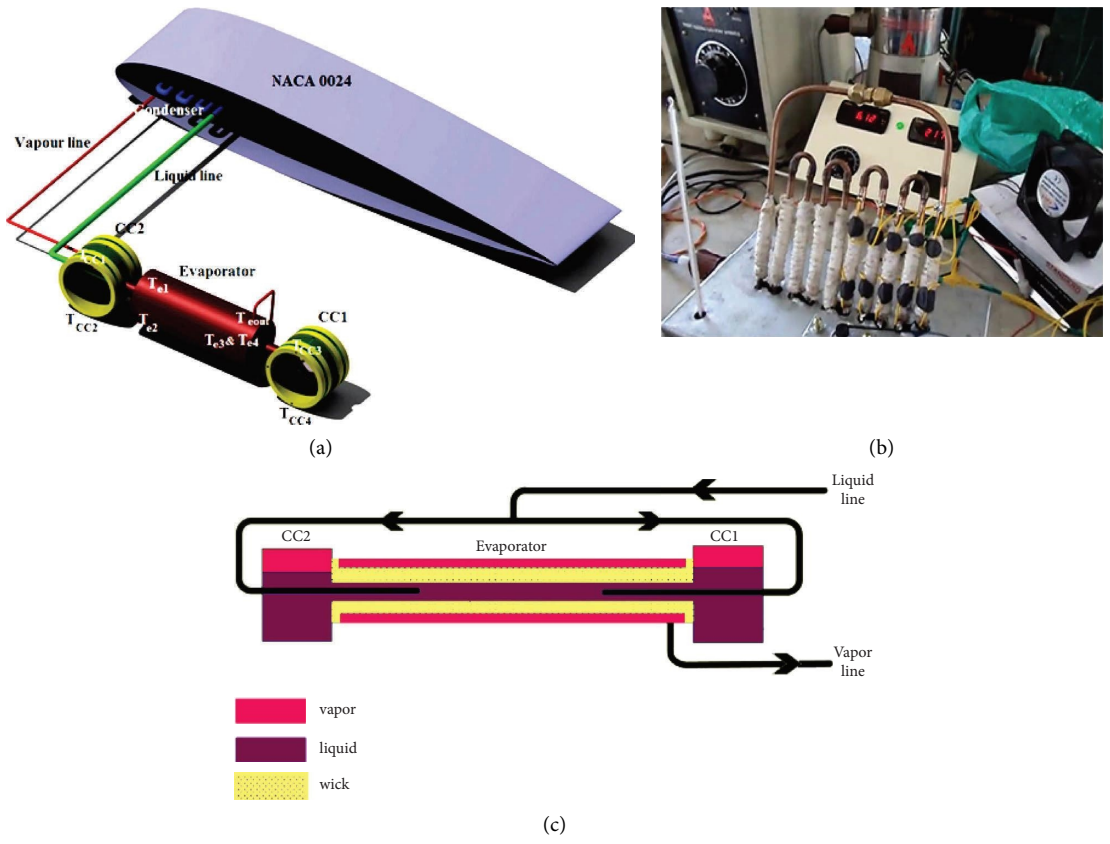

Figure 1: Experimental setup of DCCLHP system. (a) CAD model of DCCLHP. (b) Experimental setup of DCCLHP. (c) Horizontal DCCLHP layout.

2.6. Uncertainty Analysis. The thermal resistance (R) of the DCCLHP is given by the following expression:

$$R = \frac{\Delta T}{Q},$$
$$R = \frac{T_e - T_{\text{cond}}}{Q},$$
$$T_e = T_{e\_\text{Out}}, \tag{1}$$
$$T_{\text{cond}} = \frac{1}{2}\left(T_{\text{cond\_in}} + T_{\text{cond\_out}}\right).$$

The test utilized the lowest temperature of 20.5°C, with an uncertainty of 2.46%. The accuracy of the thermocouples was selected as the default value of ±0.5°C. The setup for the experiment utilized a peak current of 0.7 A and 100 A, correspondingly, with the electric potential in the power network set at 1.5 V. Likewise, the investigation into the margin of error concerning the current and voltage produced figures of 6.43% and 3.75% each, whereas the uncertainty linked to the thermal energy input was established at 7.4%. The value for the thermal resistance R was pinpointed at 7.84%.

3. Results and Discussion

3.1. Vertical Position. The temperature variations observed at significant locations along the circuit during the initiation of the DCCLHP are graphically represented in Figure 2. The evaporator's and condenser's vertical positions in the system led to them being subjected to heat loads of 5 W, 20 W, 40 W, and 80 W with respect to heat fluxes of 2.5, 5.62, 10.3, and 16.7 W/cm^2, respectively. The evaporator remained perpendicular to the condenser throughout the experiments, eliminating any adverse elevation effects. The ambient temperature of the room was recorded to be approximately 20°C. The decision not to use the fan was considered appropriate due to the comparatively low heat load of the evaporator, which remained under 100 W. An immediate temperature rise occurred while a 20 W heat load was applied to the evaporator, which can be accompanied by a noticeable temperature shift across the exchanger, indicating direct evaporation within the vapor chambers. With the fan turned off, the heat transfer process took place only by air convection from the fin-equipped aluminum plate to the surrounding air.

Figure 2(a) illustrates the fluctuations in temperature corresponding to a heat load of 5 W applied to the evaporator. It was noted that sudden spikes in the evaporator temperature occurred beyond the outlet temperature, suggesting the need for the evaporation process to be optimized within the vapor grooves. Within these specific conditions, vapor is projected to exist within the vapor channels. In case the vapor grooves get filled with liquid, a notable degree of superheat will be indispensable to start nucleate boiling in that locality. This underscores the presence of steam within the vapor pits, avoiding the need for explicit superheating to

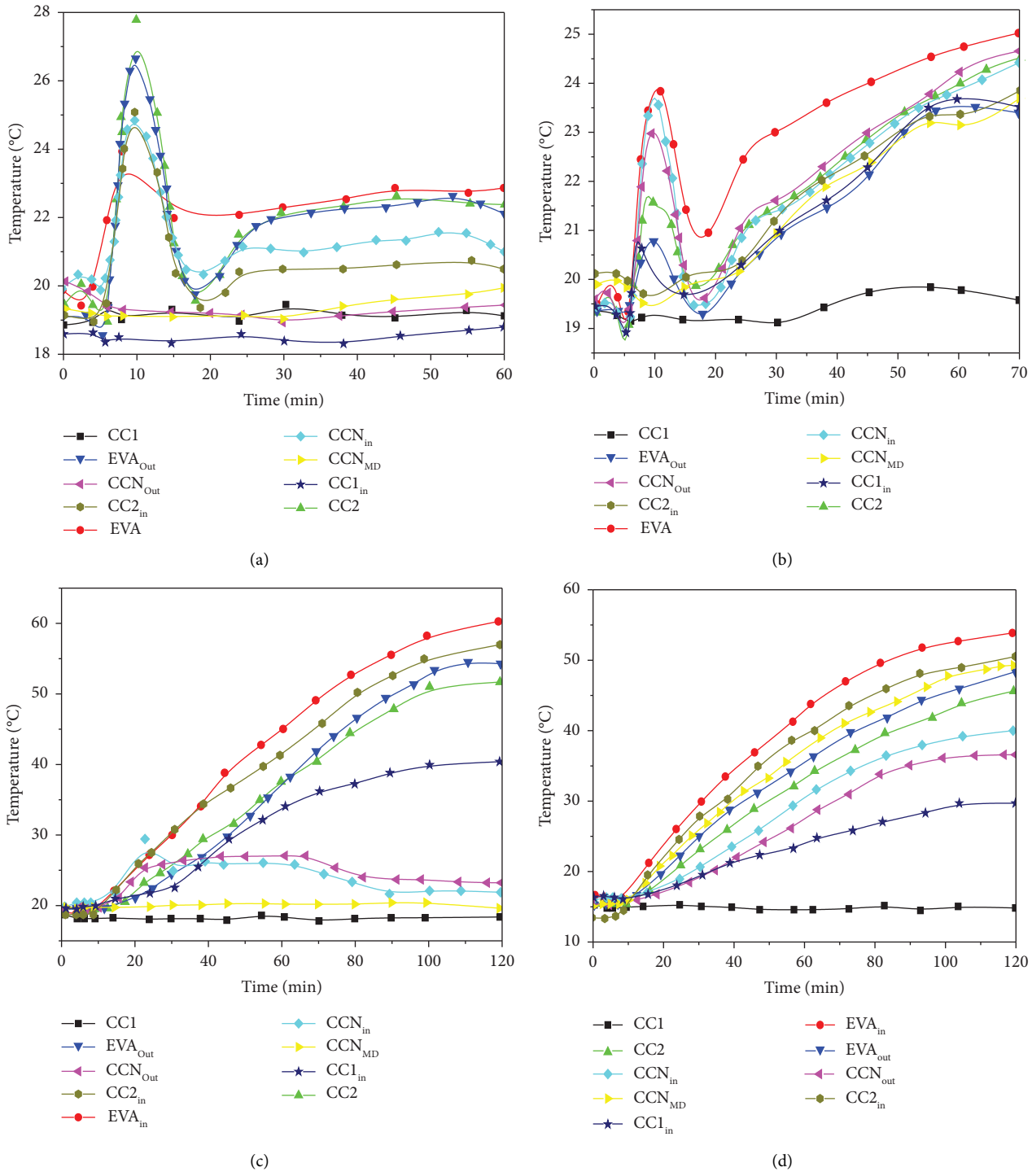

Figure 2: Temperature distributions at vertical attitude for various heat loads. (a) Startup at 5 W heat load, (b) 20 W, (c) 40 W, and (d) 80 W.

initiate nucleate boiling. Concurrently, CC2's temperature exhibited rapid ascent, consistently tracking the evaporator outlet temperature due to significant thermal leakage between the evaporator and CC2. It suggests the likelihood of vapor or gas molecules within the evaporator core, with heat leakage to CC2 manifesting as evaporation and condensation, resembling conventional heat pipe behavior. While the fluid in motion travels, the evaporator releases vapor that eventually finds its way to the condenser, resulting in a swift elevation of the condenser's surrounding temperature to match that of the evaporator's exit point. The condenser's effective dissipation of heat load to the surrounding environment upon the ingress of vapor resulted in a normalization of temperature difference and a transient peak. Remarkably, the temperature drop was strikingly evident at the center of the condenser when contrasted with the

temperature at the evaporator's exit. This particular sighting suggests a reduction in vapor penetration due to less-than-ideal condenser functionality [23].

As depicted in Figure 2(b), the introduction of a 20 W heat load to the evaporator resulted in fluctuations of the primary cycle features similar to those observed in Figure 2(a), with the startup phase progressing to phase 4 and yielding a minor peak in the outlet temperature. Upon thorough analysis, two distinct differences became evident. When the thermal burden rose from 5 to 20 W, a distinct decline in the time taken for system initialization became evident. For instance, the evaporator hits its peak temperature with a 5 W heat load after approximately 12 minutes; nevertheless, under 20 W heat loads, this duration was curtailed to around 6 minutes. Furthermore, a noticeable enhancement in the operational efficiency of the condenser was observed as the heat load increased from 5 to 20 W. The condenser's consumption efficiency remained below 50% under a 5 W thermal load but increased to over half under a 20 W heat load. The condenser's midpoint temperatures nearly resembled the evaporator output temperature after startup, which is a noteworthy observation in the system. When the steady state was exposed to a 20 W heat load, the temperature exhibited similarity to that observed under a 5 W heat load. In both scenarios, the temperature was discovered to be slightly under 25°C, indicating a consistent trend. This phenomenon can be attributed to the remarkable efficiency of the condenser in the system.

The thermal oscillations of key features within the DCCLHP loop remained consistent with the 5 W and 20 W heat loads, as demonstrated in Figures 2(c) and 2(d). Significantly, the thermal disparities observed within the DCCLHP loop underwent a magnification ranging from 40 to 80 W, which can be linked to noteworthy heat load obstacles to those experienced at power levels of 5 W and 20 W. One notable differentiation can be identified in the substantial rise in the mean operational temperature of the DCCLHP with the increase in heat load. Thermal blockage primarily emanated from the evaporator when all evaporators and CCs were positioned vertically. It is attributed to the influence of surface tension as vapor droplets from the heat exchanger's center ascend into the CC. Temperature leakage (CC2 in Figure 3) from the upper CC and from the evaporator to the lower CC was observed to be quite minimal. Figure 4 shows that after 100 minutes, the temperature of CC2 increased dramatically to about 60°C, whereas the temperature of CC1 remained constant at 20°C, leaving a large thermal differential of up to 40°C.

The DCCLHP startup process, which incorporates dual bayonet tubes, witnessed an unusual occurrence during its initial stages. Specifically, when the evaporator and CCs were oriented vertically, it was observed that the inlet temperature of CC2 closely approximated the saturation temperature of the working fluid. In the standard startup procedure of a single capillary compensation (CC) or a conventional loop heat pipe (LHP) with consistent cross-sectional areas, it is crucial to maintain the CC inlet temperature below the saturation temperature level. This condition is fundamental to guarantee the effectiveness of the cooling process and the continuous smooth operation of the LHP. Nevertheless, when examining DCCLHPs featuring dual bayonet tubes, there is a notable alteration in dynamics that leads to the emergence of a novel flow mechanism influenced by the interaction between temperature-induced circulating water and forced circulation regulated by capillary pressure. The layout of the evaporator, capillary compensators (CCs), bayonet tubes, and branches, as depicted in Figures 5(a) and 5(b), is designed in an interconnected manner to establish a self-sustaining circuit.

A noticeable temperature difference arises due to the working fluid in the fluid line segments having lower thermal conductivity than the liquid phase within the evaporator core. This circulation occurs around pressure junctions, with the inlet of CC1 playing a significant role, resulting in a localized circulation process. The local circulation pattern is primarily influenced by temperature fluctuations and becomes prominent, especially when the heat input to the evaporator is below 100 W. This circulation pattern is more likely to occur when the heat input to the evaporator remains below 100 W. However, as the volumetric flow rate of the working fluid increases to moderately significant levels at high heat inputs, capillary-driven flow within the fluid line sections surpasses the natural circulation phenomenon. The resulting counterflow effect is directed into each capillary compensator (CC) through the dual bayonet tubes, as depicted in Figure 5(b).

Upon startup, the vertical orientation presents a notable challenge for standard DCCLHPs with a single bayonet tube. This orientation can lead to startup failure, especially when the heat load is minimal, often accompanied by operational instabilities such as thermal fluctuations and reverse flow. These issues are closely connected to the energy deficit of the uppermost CC. However, dual bayonet tubes in the DCCLHP successfully mitigate operational inconsistencies, as evident in Figure 5(a), with no discernible operational destabilization observed in the study. The dual bayonet tube configuration ensures adequate cooling of both CCs from the returning subcooled liquid, allowing the upper CC to attain energy balance at a lower temperature, thus averting initial failure and associated operational instability.

3.2. 45° Angle Position. At an inclination angle of 45°, the evaporator and condenser coils of the DCCLHP are tilted, exhibiting initial heat loads of 30 and 60 watts, respectively. Figure 6 demonstrates temperature fluctuations at key locations in the loop during startup, corresponding to heat fluxes of 1.0 W/cm^2 and 1.5 W/cm^2. The experimental parameters for the DCCLHP tests remained consistent with those presented in Figures 6(a), 6(b), 6(c), 6(d). The evaporator was maintained horizontally in both condensers, and the temperature variation from the aluminum plate to the unpinned atmosphere was attributed to ambient free convection. Upon tilting the evaporator and capillary compensators (CCs) at 45°, as depicted in Figures 6(c) and 6(d), the temperature profiles at key locations along the loop during startup closely resembled those shown in the same Figures 2(c) and 2(d).

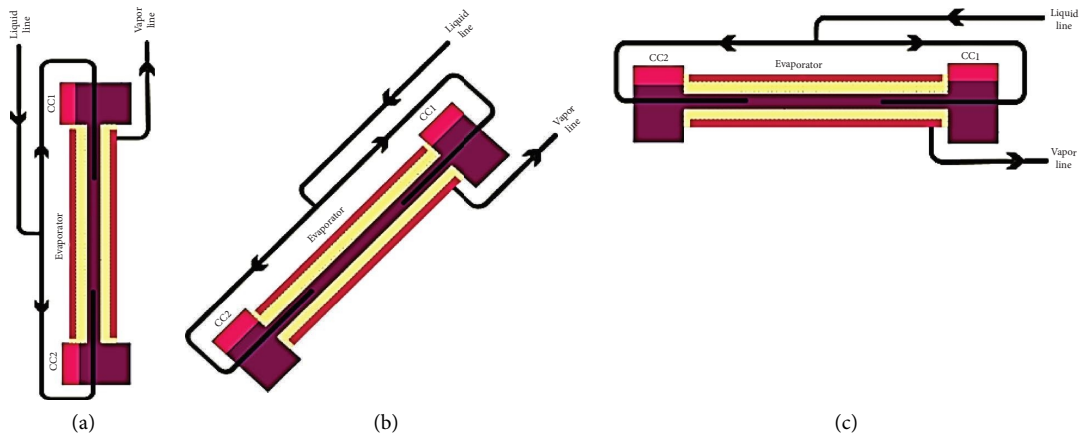

Figure 3: Evaporator positions. (a) Vertical attitude. (b) 45° tilt angle. (c) Horizontal attitude.

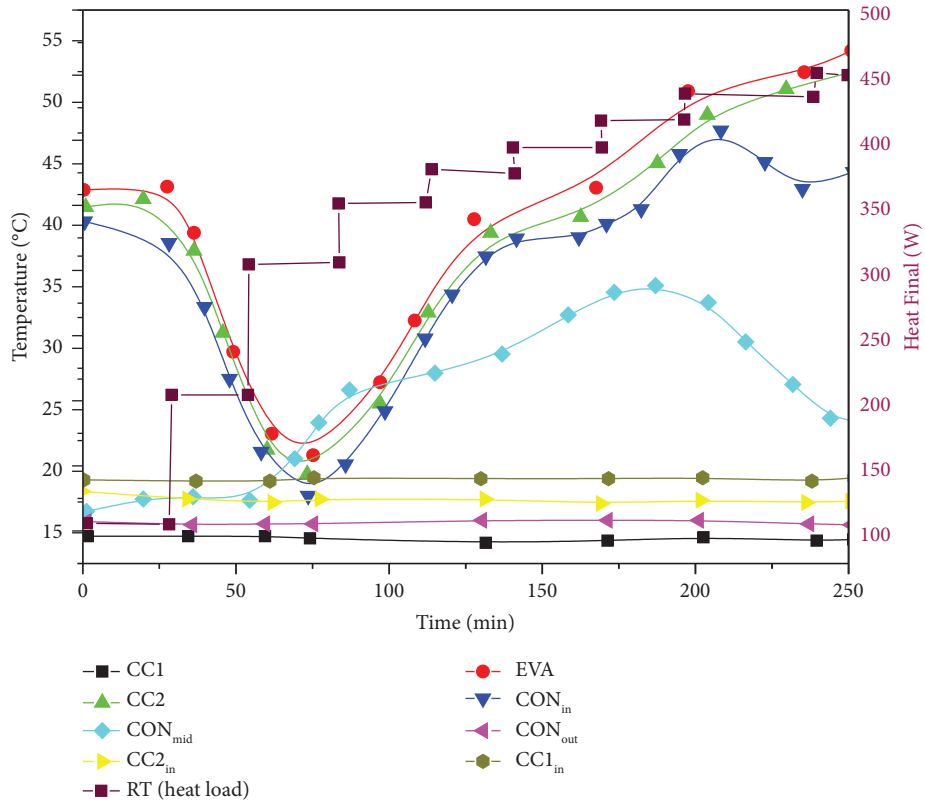

Figure 4: 45° angle orientation of DCCLHP with no adverse elevation.

The stability of the DCCLHP and successful accomplishment of the startup process can be attributed to the minimal variation observed in the temperatures of CC1, which remain relatively constant in Figures 6(a), 6(b), 6(c), 6(d). Conversely, negligible thermal leakage from the evaporator to CC1 is suggested. Conversely, the temperature of CC2 closely follows the outlet temperature, indicating substantial heat transfer from the evaporator to CC2. Simultaneously, the inlet temperature of CC2 exceeds that of CC1, in accordance with the trends delineated in Figures 2(c) and 2(d). Ultimately, the DCCLHP attains stability and accomplishes the startup process.

3.3. Horizontal Attitude. Figures 7(a) and 7(b) show that the horizontal orientation showcases temperature fluctuations at critical points in the DCCLHP loop during startup. This depiction elucidates the lateral placement of the evaporator and CCs, accompanied by initial heat fluxes measuring 30 and 60 W. Such figures align with heat fluxes of 1.0 W/cm^2 and 1.5 W/cm^2, sequentially. The DCCLHP tests' experimental conditions were maintained and consistent with those presented in Figures 2(a) and 2(b). The evaporator remained perpendicular to the condensers, and the temperature difference from the finned aluminum plate to the atmosphere was attributed to ambient convection heat

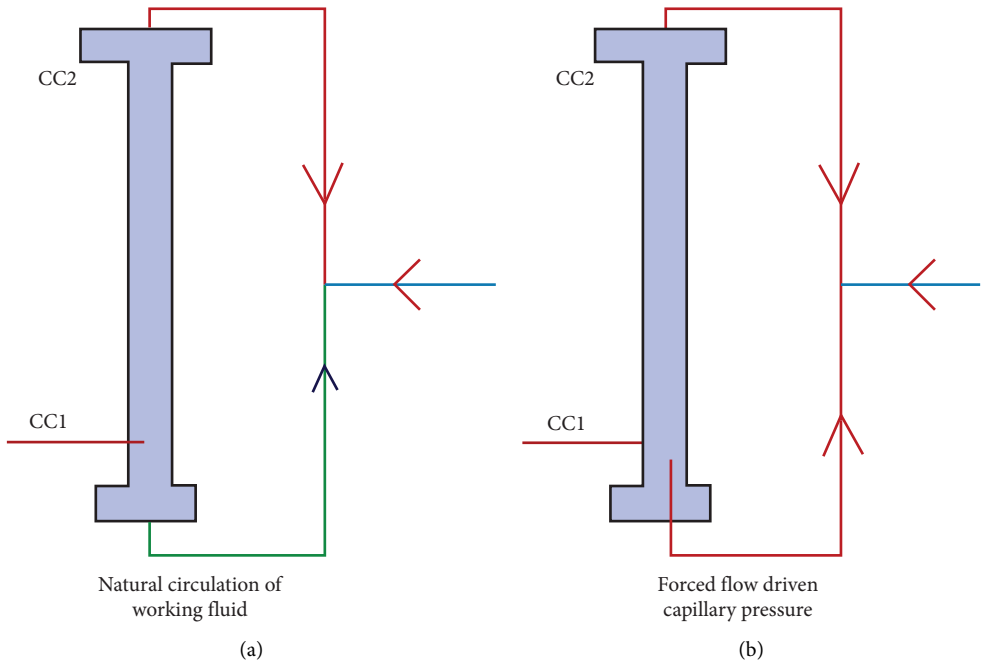

Figure 5: (a) Evaporator CCs, the bayonet tubes; (b) natural circulation.

transfer. Upon applying a thermal load of 40 watts to the evaporator, a swift escalation in both the evaporator's temperature and the outlet's temperature was detected. Immediate evaporation of the liquid occurred within the vapor chambers, with resulting vapor escaping from the evaporator, as illustrated in Figure 7(a). It is reasonable to infer the vapor's initial presence in the channels. According to Chernysheva et al. [15], the distribution of the two phases in the evaporator core/groove was in the form of liquid and vapor. This particular distribution was identified as the most favorable situation during startup.

This stands in contrast to the vertical or 45° tilted orientations where only the CC temperature corresponding to each configuration increased rapidly, while the other CCs experienced minimal changes. Another noticeable distinction is evident in Figure 7(a), where the CC2 inlet temperature remained relatively constant. In the vertical or 45° tilted orientations, it was observed that the inlet temperature of CC2 started to increase and approached the evaporator temperature. Conversely, in the horizontal configuration, the lack of gravitational force could potentially disturb the local natural circulation, ultimately resulting in the entry of capillary-pressurized subcooled fluid that was nearly identical in both CCs. The expeditious escalation in temperatures perceived in CC1 and CC2 indicates the plausible existence of gaseous or vaporous bubbles within the evaporator core. Moreover, the transfer of thermal energy from the evaporator to CC1 and CC2 is achieved via a method that bears a striking resemblance to the operation of conventional heat pipes. This particular circumstance conforms to the fourth scenario as previously scrutinized.

During this phase, the CC1 temperature consistently exceeded that of CC2, indicating unequal heat leakage from evaporation to CC1 and CC2, with CC1 experiencing higher heat leakage. As the fluid in operation circulated within the closed circuit, the vapor that emerged during the evaporation reached the condenser, causing the condensation temperature to rise rapidly above the temperature of the exit from the evaporator. Notably, the central temperature of the condenser remained significantly lower than the temperature of the exit from the evaporator, thereby signifying the minimal presence of steam and a performance level below that of the capacitor. A gradual temperature rise occurred over 45 minutes, stabilizing consistently. With a heat load of 60 W, as depicted in Figure 7(b), the temperature fluctuations at key locations along the loop closely mirrored those shown in Figure 7(a). A comparison between Figures 7(a) and 7(b) reveals that the equilibrium temperature under a 60 W heat input is lower than that under a 40 W heat load, attributed to the unique thermal conductivity of the loop heat pipe (LHP). Furthermore, the temperature rise at the midpoint of the condenser indicates an increase in the condenser's efficiency with rising heat load, leading to a decrease in the LHP's operational temperature.

3.4. Effect of Various Attitudes on Heat Transfer Characteristics of DCCLHP. Figure 8 illustrates the results of the power distinct experiment carried out on the direct contact condensation loop heat pipe (DCCLHP), showing the orientation of the evaporator/condenser cartridges in a vertical configuration. Throughout the experiment, the turbine remained consistently operational, facilitating forced air convection to cool the finned aluminum plate. It is important to note that the evaporator's midway was 0.3 m lower than the condenser's, suggesting a 0.3 m negative altitude gradient. The heat load was gradually increased in stages of W (100–400), carefully monitoring the temperature variation and values at various critical positions along the

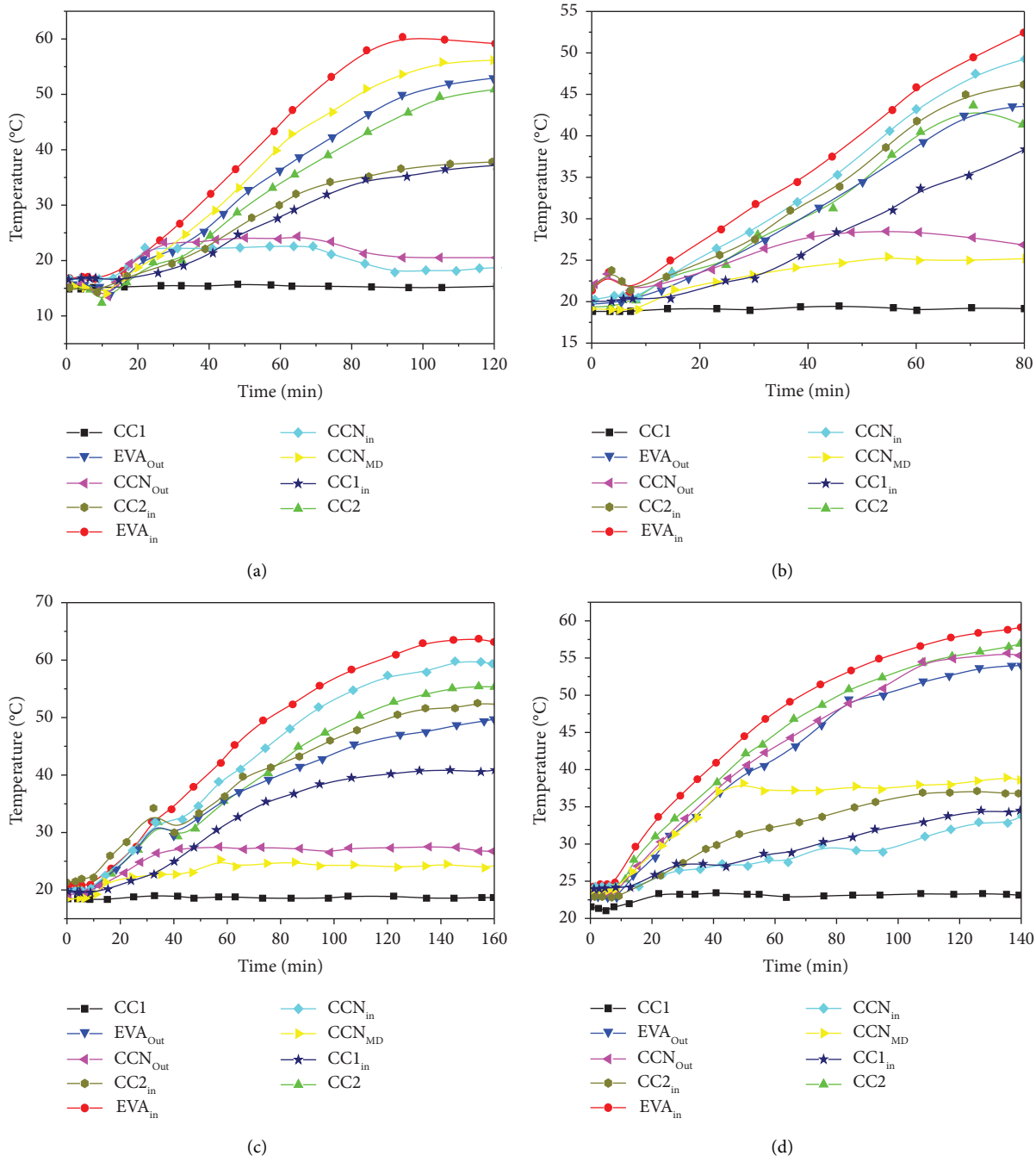

Figure 6: Temperature distributions at 45° attitude heat load. (a) Startup at 5 W heat load, (b) 20 W, (c) 40 W, and (d) 80 W.

loop. This experimental approach allowed the DCCLHP to operate in a steady-state mode at each stage of the heat load. The DCCLHP's operating temperature dropped dramatically, indicating that it was in the fluctuating permeable stage. Furthermore, the condensing unit's usage effectiveness improved as the heat load grew.

Simultaneously, the ambient temperature at the starting point of CC2 dropped significantly from 54.2°C to 26.2°C, demonstrating a change in the flow process from local spontaneous movement to forced flow, fuelled by capillary pressure-induced forced fluid velocity. After introducing a higher temperature load of 200 W, the working temperature began to climb, suggesting that the DCCLHP was now in continuous conductance mode. Notably, at 350 W, the temperature at the condenser's midpoint gradually decreased, indicating that the condenser's vapor front had contracted. The evaporator kept a constant temperature of 53°C and could tolerate a heat load of 390 W. However, at 400 W, the evaporator temperature began to climb steadily, finally reaching 60°C, with little sign of achieving a steady state, suggesting that the DCCLHP had exceeded its maximum heat transmission capacity:

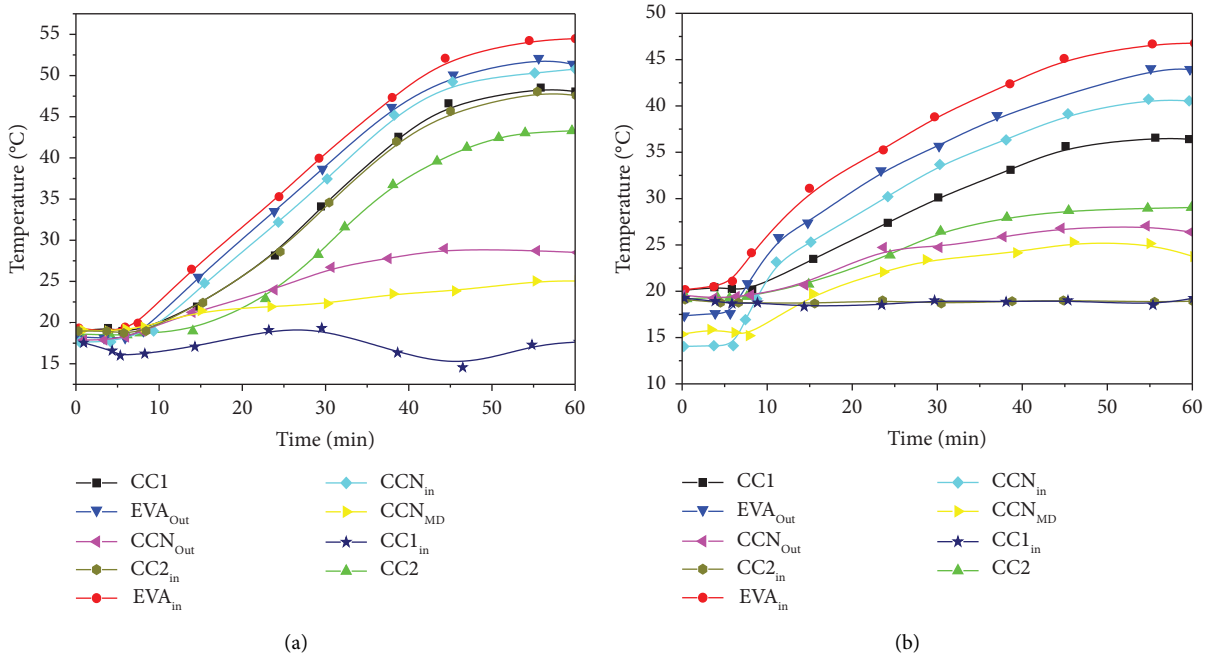

Figure 7: Temperature distributions at horizontal attitude distinct heat load (a) 40 W and (b) 80 W.

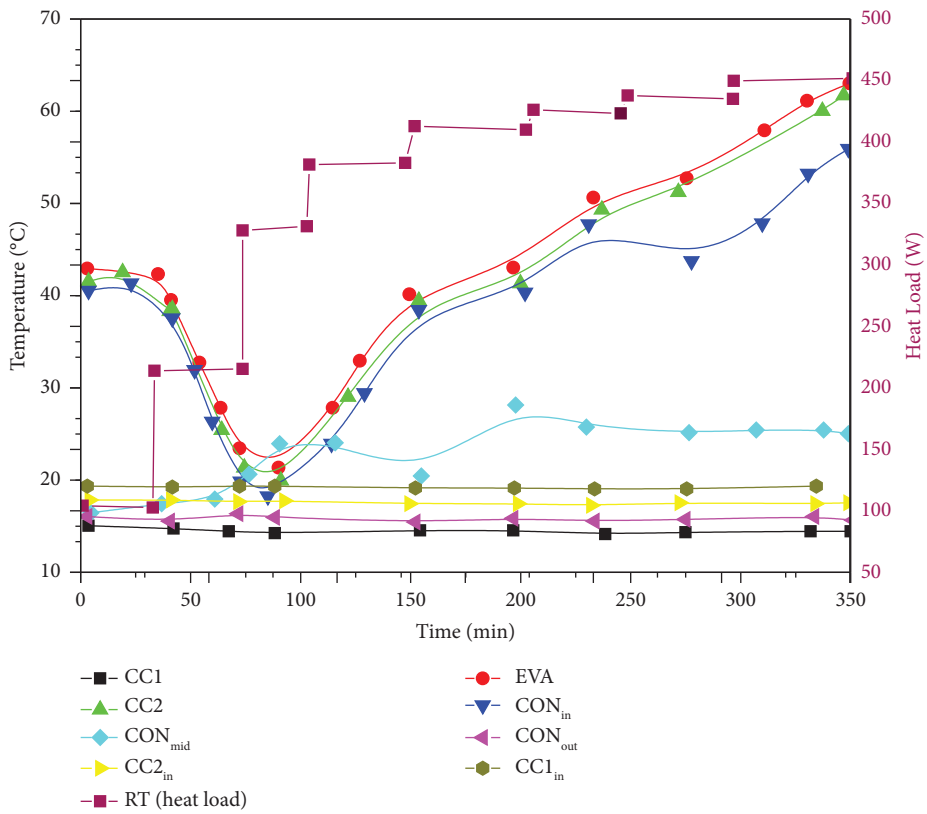

Figure 8: Vertical orientation of DCCLHP with 0.3 m adverse elevation.

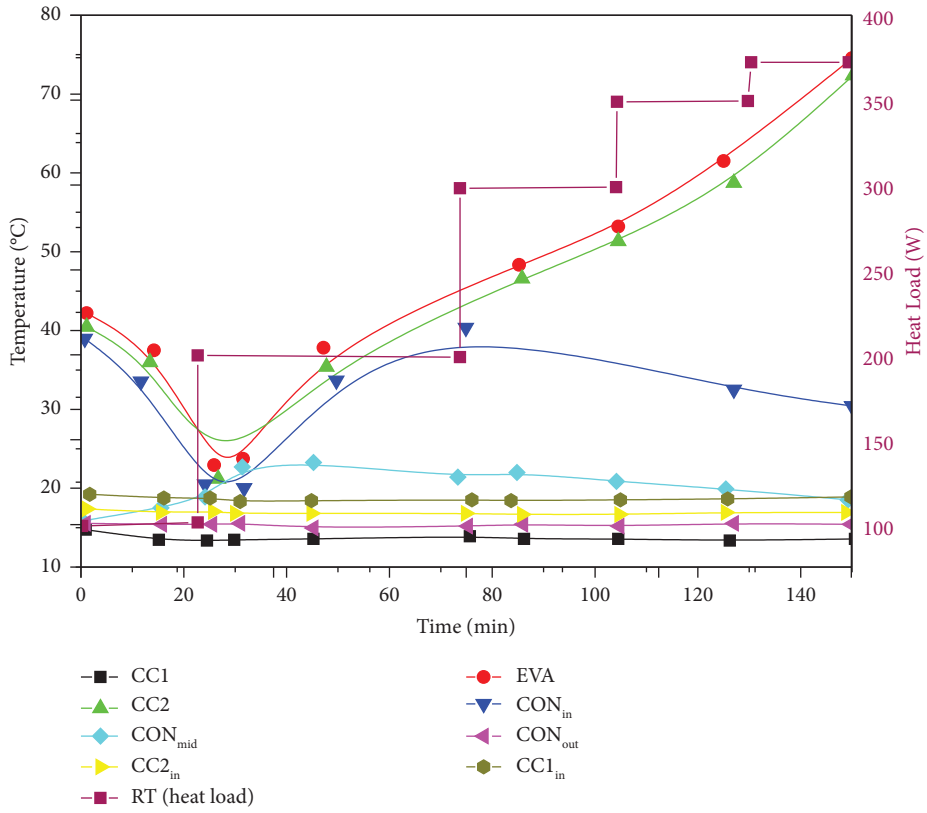

Figure 9: Horizontal orientation of DCCLHP with 0.1 m adverse elevation.

$$R = \frac{T_C - T_s}{Q_c}. \quad (2)$$

In the realm of the DCCLHP system, the thermal resistance denoted by R is a significant parameter, accompanied by T_c and T_s, symbolizing the temperatures of the evaporator and heat sink. Moreover, Q_c stands for the heat load exerted on the evaporator. Once the heat load reaches 380 W, there exists a possibility for the thermal resistance of the direct contact cooling loop heat pipe (DCCLHP) system in the vertical orientation to potentially achieve 0.081 K/W, as denoted by equation (2).

The evaporator and condenser's central points were positioned horizontally, eliminating any detrimental elevation differences. Figure 4 shows that increasing the heat load from 100 W to 200 W results in a significant reduction in operating temperature, suggesting that the DCCLHP is functioning in the variable conductance mode. Simultaneously, the temperature at the CC2 entrance dropped significantly from 42.3°C to 24.4°C, indicating a transition from localized combined convection to forced flow.

When the thermal load was elevated to 480 watts, the temperature of the evaporator persisted in rising without reaching a stable state, indicating that the DCCLHP had reached its peak heat transfer capability. When the heat load is set to 430 W, the DCCLHP system's minimum thermal resistance at a 45° tilt angle can be as low as 0.075 K/W, as illustrated in (2).

As the heat load grew to 370 W, the temperature of the evaporator gradually increased to a stable state, suggesting that the DCCLHP had attained its maximum heat transfer capability. However, the DCCLHP's heat transport capability is lower than the experimental results in Figure 9 owing to a disadvantageous elevation, which causes extra pressure to fall for the fluid in the piping system. When the heat load is 350 W, the DCCLHP system's maximum resistance to heat in the horizontal position might be as low as 0.084 K/W, as shown in equation (2).

4. Conclusion

This research presents the implementation of a dual compensation closed loop heat pipe (DCCLHP), which utilizes twin bayonet tubes. This innovation aims to address the difficulties related to initiation during situations of minimal heat loads and unfavorable circumstances. Through comprehensive experimental tests evaluating startup behavior and thermal performance under varying evaporator/CC orientations, several key insights emerge from the research data:

(1) The DCCLHP, incorporating dual bayonet tubes, effectively overcomes alignment limitations between the evaporator and CCs, enabling successful startup and operation across different orientations.

(2) Remarkably, the DCCLHP exhibits the capability to initiate operation even under extremely low heat

loads, positioning it as a promising solution for potential aviation thermal control applications in diverse environmental scenarios.

(3) An intriguing localized evaporation phenomenon is identified during tilted evaporator/CC orientations, leading to distinct temperature profiles along the loop at low heat loads.

(4) The localized natural circulation observed during tilt orientations becomes negligible when the evaporator/CCs are oriented vertically.

(5) Demonstrating impressive heat transfer efficiency, the DCCLHP achieves a notable heat transfer ability of up to 430 W over a 2.0 m distance, accompanied by a minimal thermal resistance of approximately 0.075 K/W.

The innovative DCCLHP design, coupled with its demonstrated performance enhancements, holds great potential for addressing thermal management complexities in diverse applications. Its application extends to advancements in aviation thermal control and beyond, highlighting its significance in advancing thermal control technologies.

Nomenclature

CC: Compensation chamber
DCCLHP: Dual compensation chamber loop heat pipe
LHP: Loop heat pipe
O.D.: Outer diameter
I.D.: Inner diameter
T_e: Temperature of the evaporator
T_s: Temperature of the heat sink
Q_e: Heat load exerted on the evaporator.

Data Availability

The data that support the findings of this study are available from the corresponding author upon reasonable request.

Ethical Approval

The article accurately and completely reflects the writers' research and analysis.

Conflicts of Interest

The authors declare that they have no conflicts of interest.

Authors' Contributions

P. Mohanraj performed methodology, wrote the original draft, and was involved in formal analysis. R. Sridhar was involved in experimentation, data analysis, and software. T. Gopalakrishnan was involved in supervision and formal analysis, and wrote the original draft of the manuscript. R. Manikandan performed methodology, review writing, and software. Abhijit Bhowmik was involved in supervision, funding, and review writing. All authors have reviewed the research presented and confirmed their agreement to be accountable for its accuracy and integrity.

References

[1] J. Fu, L. Bai, Y. Zhang, and G. Lin, "Experimental study on the thermal performance of a dual compensation chamber loop heat pipe with dual vapor and condenser lines," *Thermal Science and Engineering Progress*, vol. 43, Article ID 101994, 2023.

[2] L. Han, Y. Xie, J. Zhu, H. Wu, and H. Zhang, "Experimental and analytical study of dual compensation chamber loop heat pipe under acceleration force assisted condition," *International Journal of Heat and Mass Transfer*, vol. 153, Article ID 119615, 2020.

[3] Y. Qu, S. Qiao, K. Zhou, and Y. Tian, "Experimental study on the startup performance of dual-evaporator loop heat pipes," *International Journal of Thermal Sciences*, vol. 170, Article ID 107168, 2021.

[4] S. Sichamnan, T. Chompookham, and T. Parametthanuwat, "A case study on internal flow patterns of the two-phase closed thermosyphon (TPCT)," *Case Studies in Thermal Engineering*, vol. 18, Article ID 100586, 2020.

[5] Z. Zhang, H. Zhang, Z. Ma, Z. Liu, and W. Liu, "Experimental study of heat transfer capacity for loop heat pipe with flat disk evaporator," *Applied Thermal Engineering*, vol. 173, Article ID 115183, 2020.

[6] M. A. Chernysheva and Y. F. Maydanik, "Simulation of heat and mass transfer in a cylindrical evaporator of a loop heat pipe," *International Journal of Heat and Mass Transfer*, vol. 131, pp. 442–449, 2019.

[7] H. Zhang, G. Li, L. Chen et al., "Development of flat-plate loop heat pipes for spacecraft thermal control," *Microgravity Science and Technology*, vol. 31, no. 4, pp. 435–443, 2019.

[8] Q. Su, S. Chang, Y. Zhao, H. Zheng, and C. Dang, "A review of loop heat pipes for aircraft anti-icing applications," *Applied Thermal Engineering*, vol. 130, pp. 528–540, 2018.

[9] N. Watanabe, N. Phan, Y. Saito, S. Hayashi, N. Katayama, and H. Nagano, "Operating characteristics of an anti-gravity loop heat pipe with a flat evaporator that has the capability of a loop thermosyphon," *Energy Conversion and Management*, vol. 205, Article ID 112431, 2020.

[10] B. Xiao, W. Deng, Z. Ma et al., "Experimental investigation of loop heat pipe with a large squared evaporator for multi-heat sources cooling," *Renewable Energy*, vol. 147, pp. 239–248, 2020.

[11] Y. F. Maydanik, M. A. Chernysheva, and V. G. Pastukhov, "Review: loop heat pipes with flat evaporators," *Applied Thermal Engineering*, vol. 67, no. 1-2, pp. 294–307, 2014.

[12] Y. F. Maydanik, "Loop heat pipes," *Applied Thermal Engineering*, vol. 25, no. 5-6, pp. 635–657, 2005.

[13] A. Ambirajan, A. A. Adoni, J. S. Vaidya, A. A. Rajendran, D. Kumar, and P. Dutta, "Loop heat pipes: a review of fundamentals, operation and design," *Heat Transfer Engineering*, vol. 33, no. 4-5, pp. 387–405, 2012.

[14] K. Nakamura, K. Odagiri, and H. Nagano, "Study on a loop heat pipe for a long-distance heat transport under anti-gravity condition," *Applied Thermal Engineering*, vol. 107, pp. 167–174, 2016.

[15] M. A. Chernysheva, Y. F. Maydanik, and J. M. Ochterbeck, "Heat transfer investigation in evaporator of loop heat pipe during startup," *Journal of Thermophysics and Heat Transfer*, vol. 22, no. 4, pp. 617–622, 2008.

[16] K. Odagiri and H. Nagano, "Investigation on liquid-vapor interface behavior in capillary evaporator for high heat flux loop heat pipe," *International Journal of Thermal Sciences*, vol. 140, pp. 530–538, 2019.

[17] Y. Maydanik, V. Pastukhov, and M. Chernysheva, "Development and investigation of a loop heat pipe with a high heat-transfer capacity," *Applied Thermal Engineering*, vol. 130, pp. 1052–1061, 2018.

[18] H. Arya, M. M. Sarafraz, O. Pourmehran, and M. Arjomandi, "Performance index improvement of a double-pipe cooler with MgO/water-ethylene glycol (50 : 50) nano-suspension," *Propulsion and Power Research*, vol. 9, no. 1, pp. 75–86, 2020.

[19] Y. Guo, G. Lin, J. He, L. Bai, h. Zhang, and J. Miao, "Experimental study on the supercritical startup and heat transport capability of a neon-charged cryogenic loop heat pipe," *Energy Conversion and Management*, vol. 134, pp. 178–187, 2017.

[20] N. S. Ramasamy, P. Kumar, B. Wangaskar, S. Khandekar, and Y. F. Maydanik, "Miniature ammonia loop heat pipe for terrestrial applications: experiments and modeling," *International Journal of Thermal Sciences*, vol. 124, pp. 263–278, 2018.

[21] Z. Xue, W. Qu, and M. Xie, "Full visualization and startup performance of an ammonia pulsating heat pipe," *Propulsion and Power Research*, vol. 2, no. 4, pp. 263–268, 2013.

[22] G. Zhou, J. Li, and L. Lv, "An ultra-thin miniature loop heat pipe cooler for mobile electronics," *Applied Thermal Engineering*, vol. 109, pp. 514–523, 2016.

[23] L. Bai, J. Fu, G. Lin, C. Zhou, and D. Wen, "Quiet power-free cooling system enabled by loop heat pipe," *Applied Thermal Engineering*, vol. 155, pp. 14–23, 2019.

[24] J. Li and L. Lv, "Performance investigation of a compact loop heat pipe with parallel condensers," *Experimental Thermal and Fluid Science*, vol. 62, pp. 40–51, 2015.

[25] Y. Maydanik, S. Vershinin, M. Chernysheva, and S. Yushakova, "Investigation of a compact copper–water loop heap pipe with a flat evaporator," *Applied Thermal Engineering*, vol. 31, no. 16, pp. 3533–3541, 2011.

[26] Y. Zhao, S. Chang, B. Yang, W. Zhang, and M. Leng, "Experimental study on the thermal performance of loop heat pipe for the aircraft anti-icing system," *International Journal of Heat and Mass Transfer*, vol. 111, pp. 795–803, 2017.